http://dx.doi.org/10.5012/bkcs.2014.35.3.881

Photophysical Model of 10-Hydroxybenzo[*h*]quinoline: Internal Conversion and Excited State Intramolecular Proton Transfer†

Junghwa Lee and Taiha Joo*

*Department of Chemistry, Pohang University of Science and Technology, Pohang 790-784, Korea. *E-mail: thjoo@postech.ac.kr*
Received September 30, 2013, Accepted November 1, 2013

Photophysics of 10-hydroxybenzo[*h*]quinoline (HBQ) has been in controversy, in particular, on the nature of the electronic states before and after the excited state intramolecular proton transfer (ESIPT), even though the dynamics and mechanism of the ESIPT have been well established. We report highly time resolved fluorescence spectra over the full emission frequency regions of the enol and keto isomers and the anisotropy in time domain to determine the accurate rates of the population decay, spectral relaxation and anisotropy decay of the keto isomer. We have shown that the ~300 fs component observed frequently in ESIPT dynamics arises from the $S_2 \rightarrow S_1$ internal conversion in the reaction product keto isomer and that the ESIPT occurs from the enol isomer in S_1 state to the keto isomer in S_2 state.

Key Words : ESIPT, Proton transfer, Internal conversion, Time-resolved fluorescence, Anisotropy

Introduction

Molecular dynamics of ESIPT has been investigated extensively due to its fundamental importance as a model system of proton transfer in chemistry and biology.[1,2] ESIPT molecules generally show large Stokes shifts as much as 10000 cm^{-1}, which has been exploited for the applications in solar cells, sunscreens, and photosensitizers as energy conversion agents.[3,4] In addition, it is feasible to fabricate organic light-emitting diodes (OLED) showing various fluorescence colors by using ESIPT molecules.[5-7]

Reaction dynamics and molecular mechanism of ESIPT have been investigated by various time-resolved spectroscopic methods as well as quantum mechanical theories.[8-19] Two related molecules, 10-hydroxybenzo[*h*]quinoline (HBQ) and 2-(2'-hydroxyphenyl)-benzothiazole (HBT), are the benchmark systems for the study of ESIPT. Molecular structure of HBQ and its ESIPT scheme are shown in Scheme 1. We have reported accurate ESIPT rates and wave packet motions in the product states for HBQ and HBT in polar and nonpolar solvents measured by time-resolved fluorescence (TRF), which revealed detailed molecular dynamics of ESIPT.[18,20] Isotope dependence on the reaction dynamics of ESIPT has been examined as well. Surprisingly, the ESIPT rate of HBQ shows isotope dependence; the reaction proceeds in 12 ± 6 fs for HBQ and it is slowed down to 25 ± 5 fs for DBQ (deuterated HBQ), where the reactive hydrogen is replaced by deuterium.[20] Ballistic proton wave packet transfer was proposed as a mechanism for the ESIPT of HBQ based on the isotope dependence and the reaction rate, which is in strong contrast to the conventional model of the skeletal deformation assisted ESIPT.[11] In contrast, ESIPT rate of HBT was determined to be 60 fs, which is much slower than that of HBQ, with no isotope dependence. Together with the wave packet motions in the keto isomer, the results are consistent with the skeletal deformation model for HBT.[11]

In addition to the ultrafast ESIPT dynamics and population relaxation on the time scale of hundreds of picoseconds, time-resolved studies on HBQ (HBT) reported a significant contribution of a decay component with time constant of 380 (230) fs for the keto isomer, which is the reaction product.[15,18,21,22] This decay component on the intermediate time scale is solvent independent, and similar dynamics were found frequently in other ESIPT dyes as well.[23] Chou *et al*. reported 330 fs, 8-10 ps, and 300 ps decay components in the TRF of HBQ. They proposed that the $S_2 \rightarrow S_1$ internal conversion process of the keto isomer is responsible for the 330 fs component.[21] Intramolecular vibrational-energy redistribution (IVR) has also been suggested by other groups,[15,22] since coherent nuclear wave packet motions persist for more than a few picoseconds in the excited state.[11,15,18] Sanz and Douhal reported a femtosecond TRF of 2-(2'-hydroxyphenyl)-benzoselenazole, an analog of HBT molecule.[23] They observed a 230-750 fs decay component, and assigned it to the relaxation of the keto isomer through the in-plane and out-of plane vibrations. Although many TRF and transient absorption (TA) studies reported the intermediate decay component with the time constant of a few hundred femtosecond, it was attributed to the spectral relaxation of the keto isomer resulting from the vibronic relaxation and IVR processes.

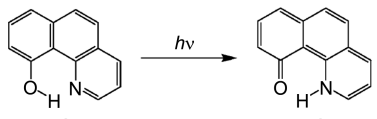

enol form keto form

Scheme 1. Molecular structure of HBQ and its ESIPT scheme.

†This paper is to commemorate Professor Myung Soo Kim's honourable retirement.

Although the intermediate decay component may have important implications on the photophysics of the ESIPT molecules and the molecular dynamics of ESIPT, it has not been actually investigated. In IVR, population of a vibrational state in a molecule is transferred to an isoenergetic state of the molecule consisting of lower frequency vibrational modes in the absence of the interaction with its environment. In contrast, vibronic relaxation refers to the population relaxation of a vibronic state via all possible channels including intramolecular processes and intermolecular energy transfer to the environment such as solvents. Although IVR and intramolecular vibronic relaxation are the energy transfer to isoenergetic states, they can cause the fluorescence Stokes shift, that is, spectral relaxation, because the energy accepting modes may have Huang-Rhys (Franck-Condon) factors different from that of the initial vibrational mode. Intermolecular processes such as solvation also cause spectral relaxation without the change of the fluorescence intensity. Internal conversion process, however, results in the fluorescence intensity change as well as the spectral change. Therefore, it is important to determine whether the intermediate decay component observed in TRF and TA is a result of the spectral relaxation, change of the transition dipole moment including its direction, or both. To this end, we have performed detailed TRF studies on HBQ including TRF spectra (TRFS) over the full emission frequency regions of the enol and keto isomers and anisotropy measurement to elucidate the origin of the intermediate decay component. HBQ was selected as our model system, because it has a rigid molecular structure with strong intramolecular hydrogen-bonding in both enol and keto isomers. Due to the rigid structure, conformational inhomogeneity in the ground state and conformational relaxation in the excited states of both enol and keto isomers, which may complicate the study, should be minimal for HBQ.[24] TRF has a unique advantage of recording excited state dynamics exclusively, whereas more popular transient absorption (TA) has contributions from ground state bleach, excited state absorption, stimulated emission and product absorption to make the analysis not straightforward.

Experimental

Details of the TRF and TRFS apparatus employing fluorescence up-conversion have been reported previously.[25] In brief, light source was a home-built cavity dumped Ti:sapphire oscillator pumped by a frequency doubled Nd:YVO_4 laser (Verdi, Coherent Inc.). Center wavelength of the oscillator output was tuned to 780 nm at the repetition rate of 380 kHz, and pump pulses were generated by the second harmonic generation in a 100 μm thick β-barium borate (BBO) crystal. Remainder of the fundamental was used as the gate pulse for the up-conversion of the fluorescence. Time resolution was estimated to be 83 fs (FWHM) assuming Gaussian pulse shape by the sum frequency generation (SFG) between the scattered pump and the gate pulses. TRFS were obtained directly without the conventional spectral reconstruction.[26-28] SFG between the fluorescence and gate pulses was performed in a 300 μm thick BBO crystal by controlling the phase matching angle of the BBO crystal, detection wavelength of the monochromator (SP300, Acton research) and the time delay stage (MTM200cc, Newport Inc.) synchronously. Group velocity dispersion (GVD) of the fluorescence collection and focusing optics, which is nonzero even with all reflective optics, and 1 mm thick fused silica window of the 100 mm sample flow cell was measured using a white light continuum. Equivalent fused silica pathlength was calculated to determine time delay of the fluorescence at each spectral point of the detected fluorescence, which in turn was used to move the time delay stage.[27] Time-resolved anisotropy was measured by rotating the polarization of the pump pulses using an achromatic half waveplate.

Methanol solution of HBQ was flown through a 100 mm pathlength flow cell to minimize photodamage. All measurements were made at ambient temperature (25 ± 1 °C).

Results and Discussion

The stationary absorption and emission spectra of HBQ in methanol are centered at 364 and 606 nm, respectively, showing Stoke shift as large as 11000 cm^{-1}.[20] The emission arises solely from the keto isomer, and the emission from the enol isomer is completely absent implying ultrafast ESIPT with a quantum yield of 1. The ESIPT rate of HBQ in methanol was reported to be 12 ± 6 fs by highly time-resolved fluorescence.[18,20] Since the ESIPT reaction involves change of the dipole moment, solvation processes of the enol and keto isomers may be significant. To differentiate the population relaxation from the spectral relaxation which may arise from the solvation, IVR, vibronic relaxation and intramolecular conformational relaxation, it is essential to measure the TRFS over the whole emission frequency region, not just the TRF at the center wavelengths of the enol and keto emissions. Since the emission wavelength of the enol isomer cannot be determined from the stationary fluorescence spectrum, approximate wavelength was guessed to perform the TRFS measurement.

TRFS measured at the emission wavelengths of the enol and keto isomers of HBQ in methanol are shown in Figure 1(a) and Figures 1(b) and 1(c), respectively. The TRFS at early times are dominated by a band centered at 460 nm, which can be assigned to the emission of the excited enol isomer. This feature is not observed in the stationary fluorescence spectrum because it is short-lived. The TRFS of the enol isomer shows an instrument limited rise to quickly reach the maximum intensity in 20-40 fs, and decays promptly. At 150 fs, the fluorescence of the enol isomer vanishes completely. This observation confirms that ESIPT is ultrafast with a quantum yield of 1, that is, all the population in the excited state of the enol isomer is transferred to other states in 150 fs. In the spectral region where the stationary emission of the keto isomer appears (Figure 1(b) and 1(c)), a broad band initially centered around 580 nm rises on a on slightly slower time scale than the 460 nm band. The 580 nm

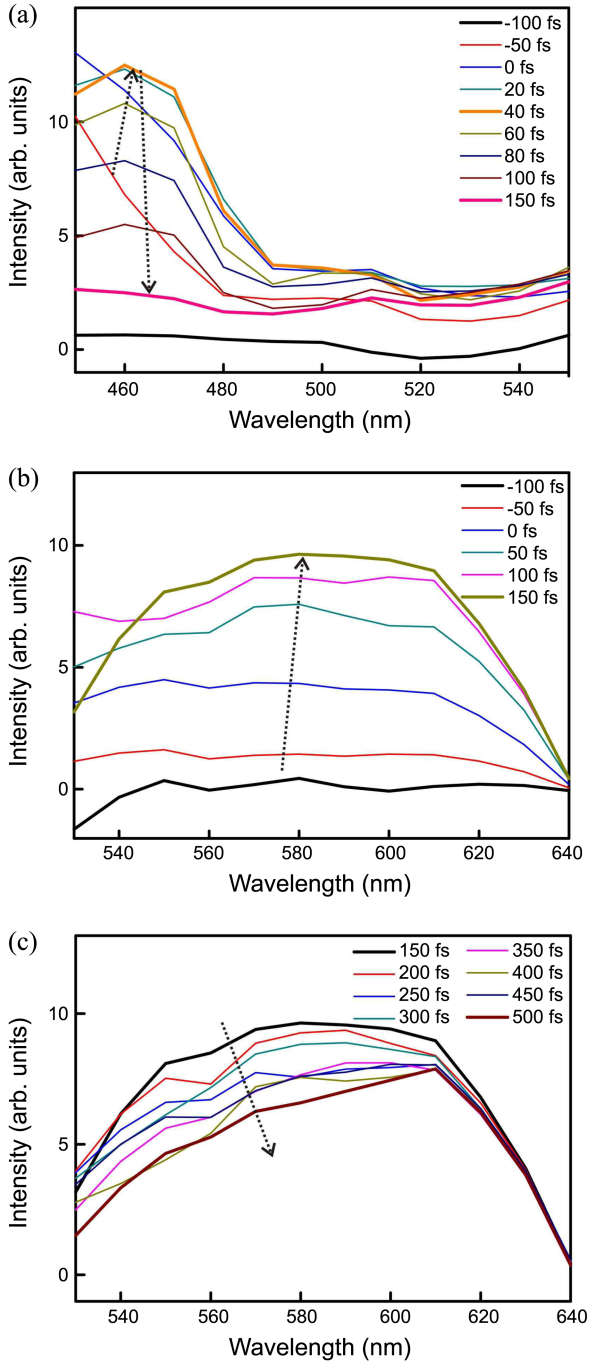

Figure 1. Time-resolved fluorescence spectra (TRFS) of HBQ in methanol around the emission wavelengths of the enol isomer (a) and the keto isomer (b, c).

band can be assigned to the emission of keto isomer. Maximum intensity is reached at ~150 fs, which is in contrast to the instrument limited rise of the enol emission. Subsequent to the ultrafast rise, the keto emission decays fast until 500 fs, which corresponds to the dynamics of intermediate time constant (380 fs) reported for the TRF of HBQ.[18] The intensity of the keto emission remains constant up to a few tens of picoseconds.

In addition to the intensity change, TRFS display the redshift (dynamic Stokes shift) of the keto emission band as

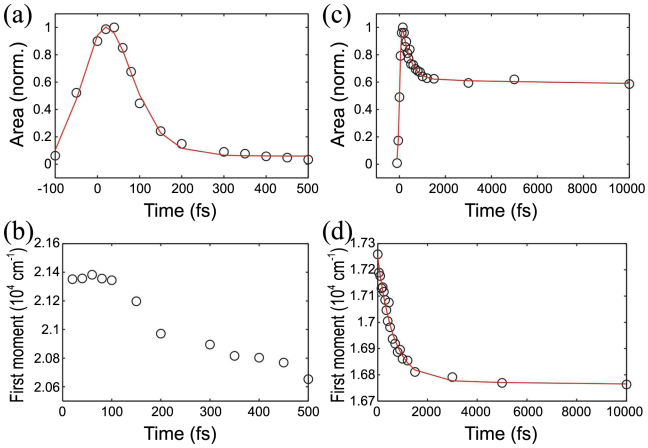

Figure 2. Area (a, c) and the first moment (b, d) calculated from the TRFS of enol (a, b) and keto (c, d) isomers. The red lines represent the exponential fits.

well. Figure 1(c) shows that high energy side of the 580 nm band decreases in intensity faster than the lower energy side resulting in apparent redshift of the emission band. In fact, a closer look of Figure 1(b) reveals the spectral redshift during the rise as well. Spectral characteristics of the TRFS were analyzed by calculating the area (integrated intensity) and the first moment, which is the average emission frequencies, of the enol and keto emission bands without any fitting routine in order to avoid the artifacts that may be introduced by the fitting.[29] The integrated intensity represents the population of an emitting species within the Condon approximation. The area and the first moment shown in Figure 2 are fitted to a sum of exponential functions, and the results are summarized in Table 1.

The integrated intensities of TRFS clearly show that the decay of the enol emission (Figure 2(a)) and the rise of the keto emission (Figure 2(c)) are ultrafast with a similar time constant, which must represent the ESIPT dynamics. The first moments (Figure 2(b) and 2(d)) show that both enol and keto emission bands undergo redshifts. Exponential fit for the first moments of the keto emission shows that the redshift proceeds by a 650 fs time constant for the most part. The solvation dynamics of methanol obtained by the dynamic Stokes shift of coumarin 153 is characterized by four time constants of 120 fs, 1.0 ps, 6.5 ps and 32 ps.[27] Considering the first three time constants, the average solvation time is calculated to be 2.5 ps. The Stokes shift of the keto emission band is significantly faster than the pure solvation dynamics. Since the observed spectral relaxation rate is a sum of rates of all processes that cause spectral relaxation, the 650 fs dynamics should reflect both solvation and additional processes such as vibronic relaxation and IVR. This can be rationalized by the fact that the keto isomer produced from the enol isomer retains large excess energy that must be released through IVR and vibronic relaxation. For a typical study of solvation dynamics, a probe molecule is excited at the red edge of the absorption band to minimize the contribution of the vibrational relaxation.[30]

Table 1. Exponential fit results for the TRFS analysis of the keto isomer and anisotropy

	A_1	τ_1 (fs)	A_2	τ_2 (ps)	A_3	τ_3 (ps)
First moment	0.92	650	0.08	7.1		
Area	0.58	360	0.52	160		
Anisotropy	0.04	310	0.21	6.0	0.15	35

More importantly, TRFS can separate the intensity (population) change and the spectral change. Figure 2(c) and Table 1 show that more than 40% of the integrated intensity of the keto emission band decreases by 360 fs time constant, which is significantly different from the 650 fs dynamic Stokes shift. That is, the intermediate decay component of a few hundred femtosecond observed frequently for the ESIPT systems reflects the population change of the keto isomer, not the results of spectral dynamics as assumed in previous reports.[15,22] Therefore we can conclude from the TRFS study that the intermediate decay component may not be the results of the vibronic relaxation, IVR or solvation, but most likely the $S_2 \rightarrow S_1$ internal conversion process.

The anisotropy at the keto emission was measured to support the conclusion drawn from the TRFS study. TRF of the keto emission at 580 nm with parallel and perpendicular polarizations between the pump and gate pulses were measured to give the anisotropy

$$\gamma(t) = \frac{I_{\parallel}(t) - I_{\perp}(t)}{I_{\parallel}(t) + 2I_{\perp}(t)}, \quad (1)$$

where the denominator is equivalent to the intensity at the magic angle (54.7°) representing the polarization independent isotropic signal. Figure 3 shows the TRF signals of the parallel and perpendicular polarizations and anisotropy. The anisotropy starts from 0.4 at time zero, which is the maximum possible value for a nondegenerate two-level system. This is surprising considering the fact that the ESIPT is faster than the instrument response. Because emission of the keto isomer is measured following the photoexcitation of the enol isomer, we are expecting the initial anisotropy to be in the range from –0.2 (perpendicular) to 0.4 (parallel) depending on the relative orientations of the transition dipole moments of the enol and keto isomers. However, it was reported that the transition dipole moments of the enol and keto isomers are nearly the same giving the initial anisotropy of 0.4 for HBQ in gas phase.[31]

The anisotropy can be described well by three time constants, 310 fs, 6 ps and 35 ps, as listed in Table 1. The 35 ps component in anisotropy can be assigned to the reorientational relaxation of HBQ in methanol by comparing the reorientational motion of molecules of similar size in methanol.[22,32] The origin of the 6 ps component can be accounted for by invoking the anisotropic reorientational relaxation of HBQ. The molecular reorientation in liquid can be highly anisotropic. For example, benzene shows sharply different reorientation rates along the spinning and tumbling motions.[33] Neat biphenyl shows 5.7 ps and 38.5 ps rotational correlation times at 58 °C corresponding to the spinning and tumbling motions, respectively.[34] One can also expect that the reorientational motion of the rigid and planar HBQ can very well be highly anisotropic. For a symmetric top molecule with the transition dipole moment lying along the symmetry axis, anisotropy in time is still single exponential. For a symmetric top molecule with the transition dipole moment perpendicular to the symmetry axis or an asymmetric top molecule, time-resolved anisotropy is biexponential.[32] For HBQ, which is an asymmetric top, biexponential reorientational relaxation is expected as observed in the experiment. Most importantly, the 310 fs component in the anisotropy decay is in excellent agreement with the 360 fs population decay of the keto isomer. Note that the relaxation along the nuclear coordinates including solvation, IVR and vibronic relaxation cannot change the electronic anisotropy. Therefore, the 310 (360) fs component should represent a change of the electronic state, which should be the internal conversion from $S_2 \rightarrow S_1$.

The schematic potential energy surfaces are presented in Figure 4 to summarize the photophysical processes in HBQ. The initial photoexcitation (upward arrow, cyan) creates the S_1 state of the enol isomer, which undergoes ESIPT to the S_2 state of the keto isomer followed by the internal conversion to S_1 in 360 fs. The ultrafast ESIPT and the $S_2 \rightarrow S_1$ internal conversion in the keto isomer require that S_2 state of the keto isomer lies below the S_1 state of enol isomer. This is quite feasible considering extremely large Stokes shift of HBQ. There are two low-lying excited singlet states, generally assigned to L_a and L_b states, with $\pi\pi^*$ character for phenanthrene analogues such as HBQ.[35] The L_a state lies higher than L_b state by 3800 cm^{-1} for phenanthrene.[36] For HBQ, the energy difference between the S_1 minimum of the keto isomer and the Franck-Condon point of initial excitation

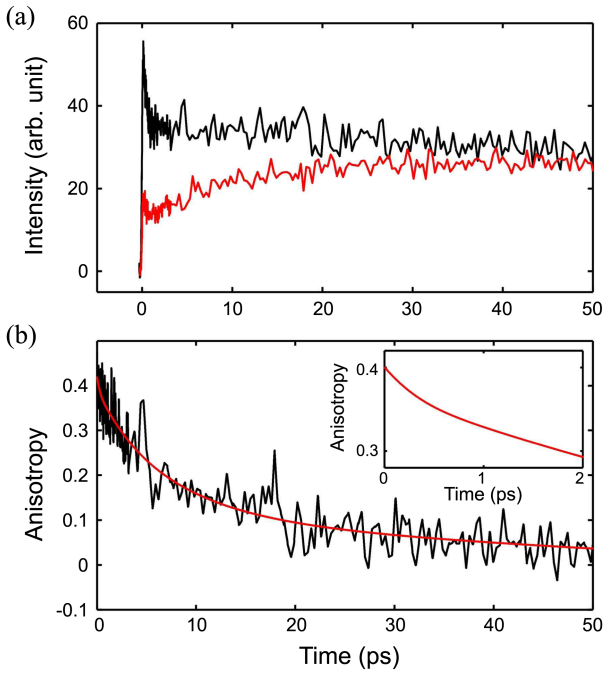

Figure 3. (a) TRF signals detected at the parallel (black) and perpendicular (red) polarizations. (b) Calculated anisotropy of HBQ at 580 nm. Red line is the exponential fit results.

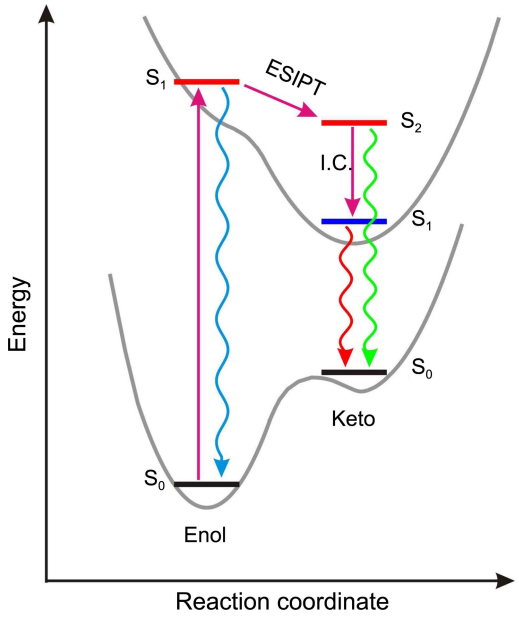

Figure 4. Schematic of the ESIPT and internal scheme. Energy are not to scale. I.C. internal conversion.

(enol) is 5660 cm^{-1}.[11] Assuming the same energy difference between the S_2 and S_1 states of the keto isomer, the S_2 state of the keto isomer lies below the initially excited enol isomer by 1860 cm^{-1}, which allows the ESIPT from the S_1 state of enol isomer to the S_2 state of keto isomer.

Conclusion

Photophysics of the ESIPT molecules such as HBQ and HBT are characterized by three time constants; ultrafast dynamics much faster than 100 fs representing ESIPT, ~300 fs dynamics of unknown origin, and hundreds of picoseconds representing population relaxation of the keto isomers. To investigate the origin of the ~300 fs dynamics, we have performed comprehensive TRF measurements on HBQ including TRFS and anisotropy at high enough time resolution to resolve all the dynamics. TRFS show that the 360 fs is due to the population relaxation of the keto isomer, not due to the spectral relaxation such as solvation, IVR, and vibronic relaxation. Anisotropy also indicates the change of the transition dipole on the same time scale (310 fs). The TRFS and anisotropy results lead to the conclusion that the 360 fs component is due to the $S_2 \rightarrow S_1$ internal conversion within the keto isomer after the ultrafast ESIPT. Therefore, the ultrafast ESIPT occurs from the S_1 state of the enol isomer to the S_2 state of the keto isomer.

Acknowledgments. This work was supported by the National Research Foundation of Korea (NRF) grant funded by the Korea government (MSIP) (2007-0056330) and the Global Research Laboratory Program (2009-00439).

References

1. Eigen, M. *Angew. Chem., Int. Ed.* **1964**, *3*, 1.
2. Chattoraj, M.; King, B. A.; Bublitz, G. U.; Boxer, S. G. *Proc. Natl. Acad. Sci. U.S.A.* **1996**, *93*, 8362.
3. Chen, D. Y.; Chen, C. L.; Cheng, Y. M.; Lai, C. H.; Yu, J. Y.; Chen, B. S.; Hsieh, C. C.; Chen, H. C.; Chen, L. Y.; Wei, C. Y.; Wu, C. C.; Chou, P. T. *ACS Appl. Mater. & Interfaces* **2010**, *2*, 1621.
4. Yang, P.; Zhao, J. Z.; Wu, W. H.; Yu, X. R.; Liu, Y. F. *J. Org. Chem.* **2012**, *77*, 6166.
5. Ma, D. G.; Liang, F. S.; Wang, L. X.; Lee, S. T.; Hung, L. S. *Chem. Phys. Lett.* **2002**, *358*, 24.
6. Kim, S.; Seo, J.; Jung, H. K.; Kim, J. J.; Park, S. Y. *Adv. Mater.* **2005**, *17*, 2077.
7. Park, S.; Kwon, J. E.; Kim, S. H.; Seo, J.; Chung, K.; Park, S. Y.; Jang, D. J.; Medina, B. M.; Gierschner, J.; Park, S. Y. *J. Am. Chem. Soc.* **2009**, *131*, 14043.
8. Elsaesser, T.; Kaiser, W. *Chem. Phys. Lett.* **1986**, *128*, 231.
9. Frey, W.; Laermer, F.; Elsaesser, T. *J. Phys. Chem.* **1991**, *95*, 10391.
10. Lenz, K.; Pfeiffer, M.; Lau, A.; Elsaesser, T. *Chem. Phys. Lett.* **1994**, *229*, 340.
11. Schriever, C.; Barbatti, M.; Stock, K.; Aquino, A. J. A.; Tunega, D.; Lochbrunner, S.; Riedle, E.; de Vivie-Riedle, R.; Lischka, H. *Chem. Phys.* **2008**, *347*, 446.
12. Lochbrunner, S.; Schultz, T.; Schmitt, M.; Shaffer, J. P.; Zgierski, M. Z.; Stolow, A. *J. Chem. Phys.* **2001**, *114*, 2519.
13. Lochbrunner, S.; Wurzer, A. J.; Riedle, E. *J. Chem. Phys.* **2000**, *112*, 10699.
14. Ryu, J.; Kim, H. W.; Kim, M. S.; Joo, T. *Bull. Korean Chem. Soc.* **2013**, *34*, 465.
15. Takeuchi, S.; Tahara, T. *J. Phys. Chem. A* **2005**, *109*, 10199.
16. Higashi, M.; Saito, S. *J. Phys. Chem. Lett.* **2011**, *2*, 2366.
17. Kim, C. H.; Chang, D. W.; Kim, S.; Park, S. Y.; Joo, T. *Chem. Phys. Lett.* **2008**, *450*, 302.
18. Kim, C. H.; Joo, T. *Phys. Chem. Chem. Phys.* **2009**, *11*, 10266.
19. Kim, C. H.; Park, J.; Seo, J.; Park, S. Y.; Joo, T. *J. Phys. Chem. A* **2010**, *114*, 5618.
20. Lee, J.; Kim, C. H.; Joo, T. *J. Phys. Chem. A* **2013**, *117*, 1400.
21. Chou, P. T.; Chen, Y. C.; Yu, W. S.; Chou, Y. H.; Wei, C. Y.; Cheng, Y. M. *J. Phys. Chem. A* **2001**, *105*, 1731.
22. Lochbrunner, S.; Wurzer, A. J.; Riedle, E. *J. Phys. Chem. A* **2003**, *107*, 10580.
23. Sanz, M.; Douhal, A. *Chem. Phys. Lett.* **2005**, *401*, 435.
24. Mohammed, O. F.; Luber, S.; Batista, V. S.; Nibbering, E. T. J. *J. Phys. Chem. A* **2011**, *115*, 7550.
25. Rhee, H.; Joo, T. *Opt. Lett.* **2005**, *30*, 96.
26. Kim, S. Y.; Kim, C. H.; Park, M.; Ko, K. C.; Lee, J. Y.; Joo, T. *J. Phys. Chem. Lett.* **2012**, *3*, 2761.
27. Eom, I.; Joo, T. *J. Chem. Phys.* **2009**, *131*, 244507.
28. Rhee, H.; Joo, T.; Aratani, N.; Osuka, A.; Cho, S.; Kim, D. *J. Chem. Phys.* **2006**, *125*, 074902.
29. Park, M.; Kim, C. H.; Joo, T. *J. Phys. Chem. A* **2013**, *117*, 370.
30. Larsen, D. S.; Ohta, K.; Xu, Q. H.; Cyrier, M.; Fleming, G. R. *J. Chem. Phys.* **2001**, *114*, 8008.
31. Schriever, C., Dissertation an der Fakultät für Physik der Ludwig-Maximilians-Universität München, 2008.
32. Fleming, G. R. *Chemical Applications of Ultrafast Spectroscopy*; Oxford University Press: New York, 1986.
33. Lee, W. I.; Shin, K. J.; Kim, M. S. *Bull. Korean Chem. Soc.* **1983**, *4*, 10.
34. Deeg, F. W.; Stankus, J. J.; Greenfield, S. R.; Newell, V. J.; Fayer, M. D. *J. Chem. Phys.* **1989**, *90*, 6893.
35. Azumi, T.; McGlynn, S. P. *J. Chem. Phys.* **1962**, *37*, 2413.
36. Parac, M.; Grimme, S. *Chem. Phys.* **2003**, *292*, 11.